Vesicle Permeabilization by Protofibrillar α-Synuclein: Implications for the Pathogenesis and Treatment of Parkinson's Disease†

Michael J. Volles, Seung-Jae Lee,‡ Jean-Christophe Rochet, Mark D. Shtilerman, Tomas T. Ding, Jeffrey C. Kessler, and Peter T. Lansbury, Jr.*

Center for Neurologic Diseases, Brigham and Women's Hospital, and Department of Neurology, Harvard Medical School, Boston, Massachusetts 02115

Received February 5, 2001; Revised Manuscript Received April 30, 2001

ABSTRACT: Fibrillar α-synuclein is a component of the Lewy body, the characteristic neuronal inclusion of the Parkinson's disease (PD) brain. Both α-synuclein mutations linked to autosomal dominant early-onset forms of PD promote the in vitro conversion of the natively unfolded protein into ordered prefibrillar oligomers, suggesting that these protofibrils, rather than the fibril itself, may induce cell death. We report here that protofibrils differ markedly from fibrils with respect to their interactions with synthetic membranes. Protofibrillar α-synuclein, in contrast to the monomeric and the fibrillar forms, binds synthetic vesicles very tightly via a β-sheet-rich structure and transiently permeabilizes these vesicles. The destruction of vesicular membranes by protofibrillar α-synuclein was directly observed by atomic force microscopy. The possibility that the toxicity of α-synuclein fibrillization may derive from an oligomeric intermediate, rather than the fibril, has implications regarding the design of therapeutics for PD.

Parkinson's disease (PD)[1] is characterized by the loss of dopaminergic neurons and the presence of fibrillar cytoplasmic inclusions called Lewy bodies in the substantia nigra. Two point mutations in the gene encoding α-synuclein (A30P and A53T), a highly expressed neuronal protein of unknown function (*1*), were identified in families with autosomal dominant early-onset PD (FPD) (*2*−*4*). Subsequently, it was demonstrated that fibrillar wild-type α-synuclein (WT) is a major component of LBs in late-onset idiopathic PD (*5*−*7*). Expression of human WT, A30P, or A53T in the brains of transgenic flies (*8*) or of human WT in the brains of transgenic mice (*9*) produced an age- and dose-dependent PD-like phenotype, suggesting a toxic gain-of-function mechanism, triggered by fibrillization (*10*, *11*). In vitro fibrillization of α-synuclein, like Aβ, proceeds via oligomeric intermediates, termed "protofibrils", that are consumed as more stable fibrils are formed (*12*−*17*). Either the α-synuclein fibril itself or a protofibrillar species could be responsible for cell death in PD (*18*). The identification of the toxic species and characterization of its mechanism of action would provide novel therapeutic targets.

Since both FPD mutations slightly accelerate in vitro oligomerization of α-synuclein, we have proposed that a protofibrillar form of α-synuclein may be pathogenic (*14*). We report here that α-synuclein protofibrils, in contrast to monomer and fibrils, tightly bind synthetic vesicles and cause transient permeabilization, a potentially toxic event. The secondary structure of the vesicle-bound protofibril (β-sheet) is distinct from the weakly bound monomer and resembles several evolved pore-forming protein cytotoxins.

EXPERIMENTAL PROCEDURES

Separation of Monomeric and Oligomeric α-Synuclein. A solution of purified recombinant (*12*) α-synuclein (1−2 mM) in PBS (10 mM phosphate buffer, 2.7 mM KCl, 137 mM NaCl, pH 7.4), prepared from lyophilized protein, was filtered through a 0.22 μm nylon spin filter (Costar). The filtrate was eluted from a Superdex 200 gel filtration column (HR 10/30) in PBS [or, in the case of membrane permeability assays (see below), in 10 mM HEPES, pH 7.4, 145 mM KCl] at a flow rate of 0.5 mL/min. Eluate was monitored at 215−280 nm, and the protein content was determined by quantitative amino acid analysis. The column was calibrated with several MW standards; protofibrillar α-synuclein and Blue Dextran 2000 eluted in the void volume.

Circular Dichroism Spectroscopy. CD spectra of monomeric and oligomeric human WT (3−10 μM in PBS), in the presence or absence of phospholipid vesicles, were measured at 22 °C using an Aviv 62A DS spectropolarimeter and a 0.1 cm cuvette. The data were acquired at 1 nm intervals, with a time constant of 4 s per measurement and a bandwidth of 1.0 nm. The final spectrum was obtained by calculating the mean of three individual scans and subtracting the appropriate background.

Preparation of Phospholipid Vesicles. PC, PG, or PC/PA (1:1 mass/mass) (Avanti Polar Lipids, Inc., Alabaster, AL)

† This work was supported by an NINDS Morris K. Udall Parkinson's Disease Research Center of Excellence Grant (NS38375), the NIA (AG14366 and AG08470), and the Alzheimer's Association Zenith Fellows Award. J.-C.R. is the recipient of postdoctoral fellowships from the Alberta Heritage Foundation for Medical Research and the Human Frontier Science Program and M.J.V. was supported by a predoctoral fellowship from the National Science Foundation.

* To whom correspondence should be addressed. Telephone: (617) 525-5260. Fax: (617) 525-5252. E-mail: plansbury@rics.bwh.harvard.edu.

‡ Current address: The Parkinson's Institute, Sunnyvale, CA.

[1] Abbreviations: AFM, atomic force microscopy; AD, Alzheimer's disease; CD, circular dichroism; EM, electron microscopy; FPD, familial Parkinson's disease; LB, Lewy body; MW, molecular weight; PA, phosphatidic acid; PBS, phosphate-buffered saline; PC, phosphatidylcholine; PD, Parkinson's disease; PG, phosphatidylglycerol; WT, wild type.

10.1021/bi0102398 CCC: $20.00
Published on Web 06/09/2001

was dissolved in chloroform or chloroform/methanol (2:1 v/v) at a concentration of 20 mg/mL. Solvent was then removed by evaporation and then lyophilization. The residual lipid was resuspended in aqueous solution [10 mM KH_2PO_4/K_2HPO_4, pH 7.4, for CD studies; 10 mM HEPES, pH 7.4, 145 mM KCl, 1 mM EDTA, 50 μM Fura-2 (Molecular Probes, Eugene, OR), for permeability studies] at a concentration of 20 mg/mL together with 100 mg/mL 1 mm diameter glass beads and incubated (25 °C, 2 h) to produce large multilamellar vesicles. More uniform vesicle populations were formed by passing these through a nuclepore polycarbonate track-etch membrane (Whatman, U.K.) with a defined pore size (80 nm for CD studies, 100 nm for permeability studies) at least 13 times (Avanti Mini-Extruder, Avanti Polar Lipids) (*19*). Alternatively, vesicles were sequentially filtered through a 200 nm filter, followed by 100 and 30 nm filters, to isolate fractions with progressively smaller diameters. Vesicles encapsulating dye were separated from free dye by gel filtration using PD-10 columns (Amersham Pharmacia Biotech, Uppsala, Sweden) and were stored in the dark at 4 °C. Vesicle size (see Figure 5C) was analyzed by electron microscopy (EM) with negative staining (1% uranyl acetate). A distribution of vesicle sizes was observed, with a mean slightly larger than the nuclepore membrane pore size.

Membrane Binding Assay. Freshly purified α-synuclein (5 μg) was incubated with 0.5 mg of synthetic vesicles for 2 h at room temperature in 400 μL of PBS. Membrane-bound and free α-synuclein were separated by membrane flotation (Figure 2) (*20*). The binding reaction was mixed with 0.42 mL of 60% iodixanol gradient medium (Life Technologies, Inc.) and overlaid with 2.5 mL of 25% iodixanol and 0.1 mL of 5% iodixanol in PBS. The step gradient was centrifuged for 2 h at 200000*g* in an SW55 rotor (Beckman) at 4 °C. Western blotting was performed as described in Lee et al. (*21*) using LB509 (Zymed Laboratories Inc., South San Francisco, CA) as the primary antibody.

Surface Plasmon Resonance Detection of Vesicle Binding. Extruded PG vesicles (100 nm) were preadsorbed to a Pioneer Chip L1 (BIAcore) to saturation (*22*), and the surface was stabilized by removing partially adsorbed material with HEPES-buffered saline (HBS) (pH 7.4, 100 μL/min for 10 min). Protein binding to vesicles was monitored on an upgraded BIAcore 1000 instrument at 2 μL/min in HBS (pH 7.4, 25 °C, 1 h). Subsequently, the protein-containing buffer was replaced with HBS, and protein dissociation was measured at 100 μL/min. Binding of protofibrils (5 μM α-synuclein) was contrasted to monomer (5−50-fold concentration excess) and fibril (10-fold concentration excess).

Membrane Permeability Measurements. The method of Blau and Weissmann (*23*), measuring the fluorescence of a calcium-sensitive fluorophore (Fura-2), entrapped in vesicles, was utilized. A fluorescence detector based on the common stopped-flow device was assembled. The flow cell of an HPLC fluorescence detector [Kratos (Chestnut Ridge, NY) FS 950 Fluoromat with F4T5BL lamp; excitation filter, 334 nm with 10 nm band-pass; emission filter, long-pass with 495 nm cutoff] was connected to the central port of a T-type mixing chamber, the remaining two ports of which were connected to 100 μL syringes. A solution of vesicles (50 μL) in one syringe and 50 μL of solution containing 10 mM $CaCl_2$ and α-synuclein in the other, were rapidly mixed in the flow cell. Alternatively, solutions were mixed in a plastic tube, and aliquots were injected through the fluorescence detector using an HPLC pump (Waters 600E). The carrier solvent was 10 mM HEPES, 145 mM KCl, and 5 mM $CaCl_2$, pH 7.4, at 0.5 mL/min. For gel filtration analysis, the solutions were mixed by hand, incubated for 30 min, and injected onto a Sephadex G25 medium column (HR 10/30) equilibrated at 0.5 mL/min with 10 mM HEPES, 145 mM KCl, and 5 mM $CaCl_2$, pH 7.4. The chromatography system consisted of a Waters 2790 HPLC, a 996 PDA detector (Waters), and a Kratos Fluoromat in series.

Perturbation of Preadsorbed Lipid Membranes. A 5 μL aliquot of a suspension of 100 nm PG vesicles (containing 0.5 mM $CaCl_2$) was deposited on a freshly cleaved mica substrate (pelco mica, Ted Pella Inc., Redding, CA). After initial expansion, the droplet retracted and came to equilibrium usually within 30 s. A 3 μL aliquot containing either monomeric α-synuclein (100 μM, filtered through a 0.02 μm filter, Whatman anotop 10, Meadstone, England; the absence of protofibrils was confirmed by AFM) or incubations of the above solution (several days at 37 °C) was carefully injected into the droplet, using a micropipet with a gel-loading tip. The droplet was left on the surface for ca. 2 min before being displaced with 150 μL of Millipore water. The surface was gently dried and imaged in air immediately by AFM as in Conway et al. (*14*).

Electron Microscopy of Vesicle Perturbation. PG vesicles were incubated for 30 min exactly as described above in the Membrane Permeability Measurements section. After the incubation period, 5 μL of the solution was spotted onto a glow discharged formvar carbon-coated grid for 1 min and then stained for 1 min with 1% uranyl acetate. Samples were analyzed using a JEOL 1200EX transmission EM at 80.0 kV.

RESULTS

Isolated α-Synuclein Protofibrils Are Metastable β-Sheet-Rich Oligomers. Protofibrillar α-synuclein, formed upon solubilization of lyophilized recombinant α-synuclein, was separated from monomeric protein by gel filtration chromatography (Figure 1A). Analysis of the void volume fraction by AFM showed predominantly spherical species with a diameter and height of ca. 4 nm (Figure 1B) (*13*). No chainlike protofibrils or mature fibrils were detected. However, after incubation, elongated protofibrils (*12*) and, eventually, fibrils were formed. In contrast to monomeric α-synuclein, which is "natively unfolded" (*24*), the spherical protofibrils produced a circular dichroism (CD) spectrum characteristic of a predominance of β-sheet structure (Figure 1C, left panel; note difference from predominantly helical spectrum in right panel) (*12*). Reinjection of the void volume peak led to some repopulation of the monomer, demonstrating that the spherical protofibrils are unstable to dilution. Incubation of the pure monomeric fraction led to a steady increase in the void volume peak (until it represented ca. 5% of the total protein), followed by its disappearance as the more stable fibrils formed (*25*).

Vesicle-Bound Forms of Protofibrillar and Monomeric α-Synuclein Are Distinct. As previously reported (*26*), monomeric α-synuclein assumed some α-helical structure upon binding anionic synthetic vesicles (Figure 1C, right

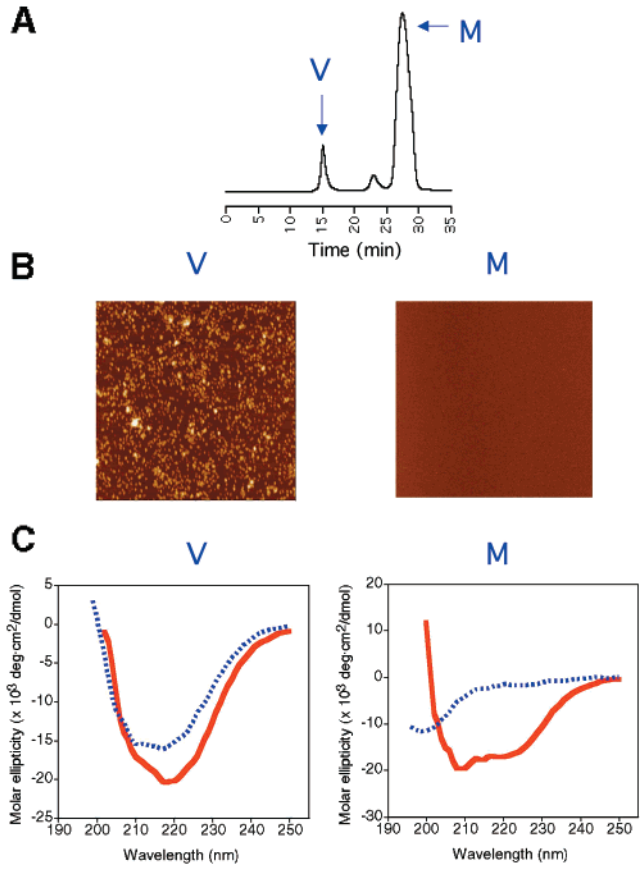

FIGURE 1: Characterization of monomeric (M) and protofibrillar (V) α-synuclein in solution and bound to phospholipid vesicles. (A) Gel filtration chromatogram showing separation of protofibrils (V) from monomer (M). (B) AFM images (2 μm^2) of the fractions containing isolated protofibrils (spherical structures at left, height = 2−4 nm) and the monomer (right). α-Synuclein monomer was not adsorbed or was too small to be detected. (C) CD spectra of the protofibrils (left) and the monomer (right) in the absence (blue dashed) or presence (red solid) of an approximately 20-fold excess (w/w) of 1:1 POPC/POPA (1.25 mg/mL) vesicles.

panel). In contrast, α-synuclein protofibrils, when bound to the same vesicles, produced a β-sheet CD spectrum resembling that of the unbound protofibrils (Figure 1C, left panel). Protofibril binding was confirmed by separately incubating monomer and protofibril with acidic [PC/PA (1:1) or PG] or neutral (PC only) synthetic vesicles. The vesicle-bound and free proteins were separated by density-gradient flotation centrifugation (Figure 2A) and analyzed by SDS−PAGE (detected by Western blotting using LB509). Consistent with a previous report (*26*), monomeric α-synuclein binds to acidic phospholipids (PG or PC/PA) but not to neutral ones (PC, Figure 2B). Protofibrillar α-synuclein showed a similar binding preference (Figure 2B; note that these blots could not be interpreted quantitatively, since the transfer efficiency and the epitope availability are expected to differ between the monomeric and protofibrillar forms). Under identical conditions, but using brain-derived vesicles instead of synthetic vesicles, protofibrillar α-synuclein was observed to bind much more avidly than the monomer (Lee et al., unpublished results).

High-Affinity Vesicle Binding Is Specific to Protofibrillar α-Synuclein. Selective binding of protofibrillar α-synuclein to PG vesicles was measured under the conditions of surface plasmon resonance, using chips to which PG or PC vesicles had been stably adsorbed (*22*). It is important to note that in this experiment, as compared to the sedimentation experiment described above, far less vesicle surface area is available for binding. Binding was only observed to PG vesicles and was clearly strongest (i.e., greatest amount of protein bound) in the case of protofibrillar α-synuclein, as compared to monomeric and fibrillar proteins (Figure 2C). The difficulty in dissociating vesicle-bound protofibrils (monitored for 1 h) was indicative of a very slow off rate, inconsistent with reversible, helix-mediated binding such as that demonstrated by the exchangeable apolipoproteins (*26*). A quantitative analysis of binding affinity was not possible, since the protofibrillar fraction is heterogeneous and the protofibril concentration (in terms of moles of protofibrils) is unknown (because the number of α-synuclein molecules constituting the average protofibril is unknown). However, a crude estimate yields an approximate affinity constant in the low nanomolar range. Such strong binding is consistent with protofibril insertion into the lipid bilayer. Finally, the amount of binding was saturable and dependent on the α-synuclein concentration, and the two mutant proteins, A53T and A30P, demonstrated a similar level of binding, on a per mole basis, to the WT protein.

Only Protofibrillar α-Synuclein Permeabilizes Synthetic Vesicles. To investigate the effect of protofibril binding on vesicle integrity, synthetic PG or PC vesicles (approximate diameter of 150 ± 50 nm) were loaded with Fura-2, a calcium-sensitive fluorescent dye (*23*). α-Synuclein in monomeric, protofibrillar, or fibrillar form and calcium were added to the extravesicular space, and enhanced fluorescence from calcium-bound Fura-2 was monitored. The chelating calcium ionophore ionomycin, which allows calcium to passively diffuse through the vesicular membrane, rapidly produced the theoretical maximal increase in fluorescence intensity (ca. 3-fold) (see Figure 3A). Addition of monomeric α-synuclein (26 μM) to PG vesicles produced no fluorescence enhancement, while addition of a significantly lower concentration of protofibrillar α-synuclein (4 μM, in terms of moles of monomer) to the same vesicles produced a significant signal within minutes (Figure 3A). Addition of protofibrils to vesicles that did not contain Fura-2 did not produce any change in the signal, demonstrating that the increase due to protofibril addition (Figure 3) was not due to light scattering by vesicles or protofibrils. No permeabilizing effect was measured on addition of fibrillar synuclein (30 μM α-synuclein) to PG vesicles (Figure 3B) or on addition of monomeric or protofibrillar α-synuclein to PC vesicles. Finally, as compared to WT, both mutant proteins, A53T and A30P, demonstrated comparable protofibril-specific permeabilizing activity per mole of α-synuclein.

The magnitude of the permeabilizing effect was α-synuclein concentration-dependent and saturable at between 15% and 60% of the ionomycin effect, suggesting that a subpopulation of Fura-2-containing vesicles may be immune to permeabilization. This theory is supported by the fact that the maximal effect depended on PG vesicle size (Figure 3D). The smallest vesicles (average diameter of ca. 30 nm) were most prone to permeabilization (ca. 62% of the ionomycin effect). This size dependence could reflect membrane curvature or the fact that the smaller vesicles are more likely to be unilamellar.

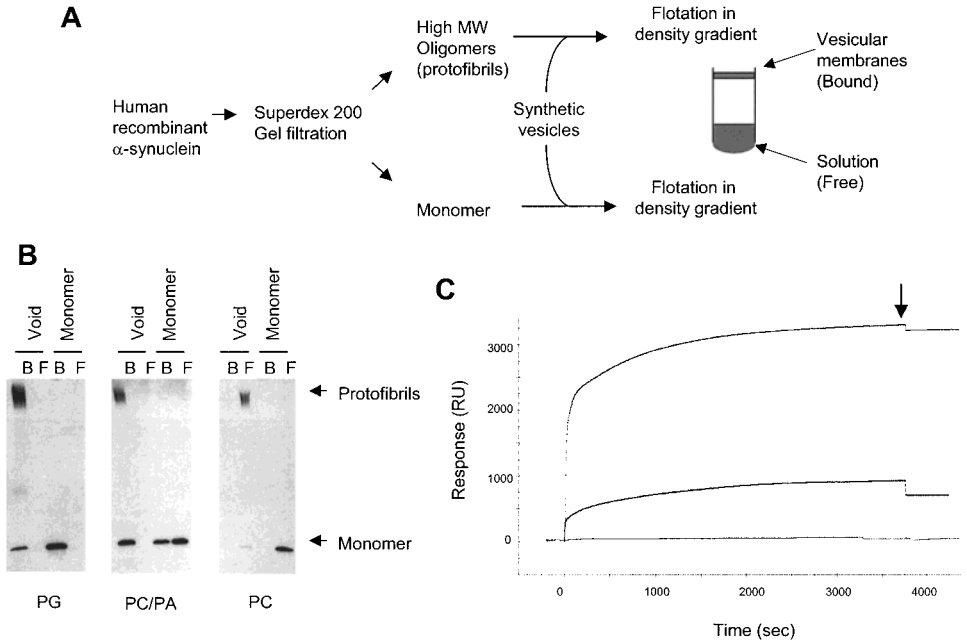

FIGURE 2: Binding of α-synuclein monomer, protofibrils, and fibrils to synthetic vesicles. (A) Protofibrils and monomer were incubated with synthetic vesicles. Membrane-associated proteins were separated from free proteins by density-gradient centrifugation. (B) The membrane-bound fraction (lane B) and free fraction (lane F) were analyzed by Western blotting with monoclonal antibody LB509. SDS-stable high molecular weight protofibrils were found in void volume samples, along with a small amount of dissociated monomers. Note that both the monomer and protofibrils preferentially bind to the phospholipid vesicles with acidic headgroups (egg PG and POPC/POPA as opposed to POPC). (C) Surface plasmon resonance demonstrates the high-affinity binding of protofibrils to egg PG vesicles. After vesicle adsorption to create a stable surface (not shown), α-synuclein in protofibrillar (upper trace, 5 μM), monomeric (bottom trace, 50 μM), or fibrillar (middle trace, 50 μM) was added (buffer blank is also shown in the bottom trace and is indistinguishable from monomer). After binding had saturated, the protein solution was replaced with buffer (wash phase, see arrow), but very little dissociation of bound protofibril was observed (signal did not change over 1 h).

Permeabilization by α-Synuclein Protofibrils Leaves Most, If Not All, Vesicles Intact. To test whether the increased fluorescence resulted from vesicle lysis or permeabilization, the Fura-2-loaded PG vesicles were analyzed by gel filtration, before and after various treatments. Treatment with Triton X-100 lyses 100% of the vesicles, and Fura-2 fluorescence was detected primarily in the fractions that correspond to the soluble calcium−Fura-2 complex (Figure 4A). By comparison, ionomycin produced a comparable increase in the total fluorescence, all of which remained in the vesicle-entrapped fraction (Figure 4A). After incubation with α-synuclein protofibrils, fluorescence was increased in the vesicle fraction (Figure 4B) and, to a lesser extent, in the free calcium−Fura-2 fraction (arrowhead). The simplest explanation for this mixed effect is that protofibrils transiently permeabilize some of the vesicles in this population, perhaps via large nonselective pores or local membrane disruptions (*27*), allowing calcium influx *and* Fura-2 efflux.

Fragmentation of Adsorbed PG Membranes by α-Synuclein Required Its Incubation/Oligomerization. PG vesicles were preadsorbed onto mica, and subsequently, solutions of prefiltered, monomeric α-synuclein (100 μM) that had been preincubated for various times were added (direct adsorption of PG vesicle-bound α-synuclein protofibrils produced an erratic surface). At the earliest time point, intact adsorbed vesicle membranes were detected (Figure 5A). However, after preincubation of the α-synuclein (9 days at 37 °C), membrane fragmentation was clearly observed (Figure 5B). The time dependence of the membrane-perturbing effect is consistent with the involvement of protofibrillar α-synuclein. A morphological change in vesicle structure, induced by α-synuclein, was also observed by EM (Figure 5C,D). A previous report notes that a qualitatively similar phenomenon is produced by α-synuclein that is presumed to be monomeric (*28*). Due to vesicle disruption, we were unable to directly image membrane-bound protofibrillar α-synuclein.

DISCUSSION

The correlation between fibrillar α-synuclein (Lewy bodies) and cell death in Parkinson's disease appears to reflect a causal link (*8*, *9*, *29*). The nonfibrillar nature of the α-synuclein deposits in the brains of the "symptomatic" transgenic mice (*9*), our own studies of α-synuclein fibrillization (*25*), and studies of PD brain (*30*) each suggest that a protofibril could be the pathogenic species (*18*).

Since the clear difference between PD brain and normal brain is not the primary structure of α-synuclein (the great majority of PD cases involve WT) but its quaternary structure, any potentially neurotoxic property of α-synuclein that is selectively expressed in vitro by the protofibrillar form is a candidate to account for toxicity in PD. We demonstrate here that the conversion from monomer to protofibril involves a secondary (as well as quaternary) structural transition from natively unfolded (random coil) (*24*), to predominantly β-sheet, also the predominant secondary structure of the product amyloid fibril (*12*). While binding of monomeric α-synuclein to membranes has been consistently observed (*26*, *31*), binding of the protofibrillar form has not been reported. The secondary structural consequences of binding on the two forms are quite different, with the bound monomer assuming helical structure (*26*) while the

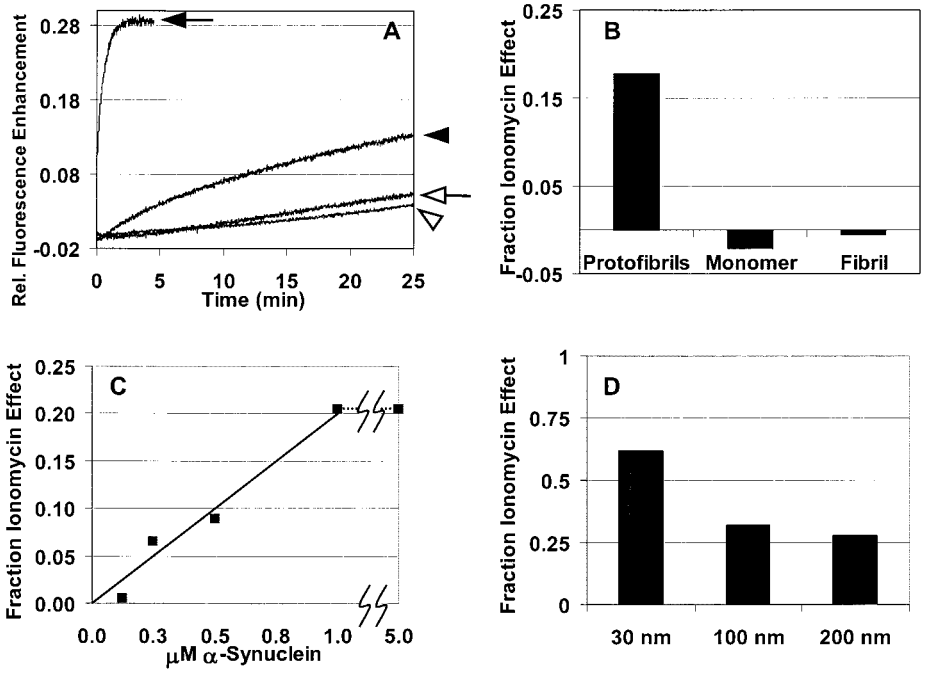

FIGURE 3: Effects of α-synuclein in various oligomeric states on the permeability of egg PG vesicles. A protein or buffer solution was mixed with Fura-2-loaded 100 nm PG vesicles as described in the text, and the enhancement of fluorescence was measured (A). The outlined arrowhead points to the negative control (buffer) trace. The outlined arrow and black arrowhead point to the monomeric (26 μM) or protofibrillar α-synuclein (4.2 μM) traces, respectively. Each trace is the average of two or more experiments. The ionophore ionomycin (black arrow, 31 nM) produced the theoretical maximum fluorescence enhancement. The shallow positive slope of the monomer and buffer traces is due to a finite background level of calcium or Fura-2 flux across the unperturbed membrane. Twenty minutes after addition of protofibril, the slope, which is initially significantly steeper than that of the buffer or monomer trace (due to a greater calcium flux rate), decreases to near the background level, indicating that the initial calcium flux has come to equilibrium. In (B), a comparison of the maximal effects of monomeric (31 μM), protofibrillar (5 μM), and fibrillar (30 μM) α-synuclein is shown. Effects are reported as fractions of the ionomycin effect and represent the average of two measurements. Measurements were made after the protofibril-induced calcium flux had come to equilibrium (~15 min). (C) The permeabilizing effect is concentration-dependent and saturable, as shown in the graph of membrane permeabilization of 100 nm egg PG vesicles by WT protofibrils as a function of concentration. Each point represents the maximum signal obtained (expressed as a fraction of the ionomycin signal) at the given concentration during a time course such as that shown in (A). (D) The magnitude of the permeabilizing effect of protofibrils depends on vesicle diameter. The *y*-axis reports the fraction of the maximum (ionomycin) effect produced by WT protofibrils. This experiment is representative of several trials.

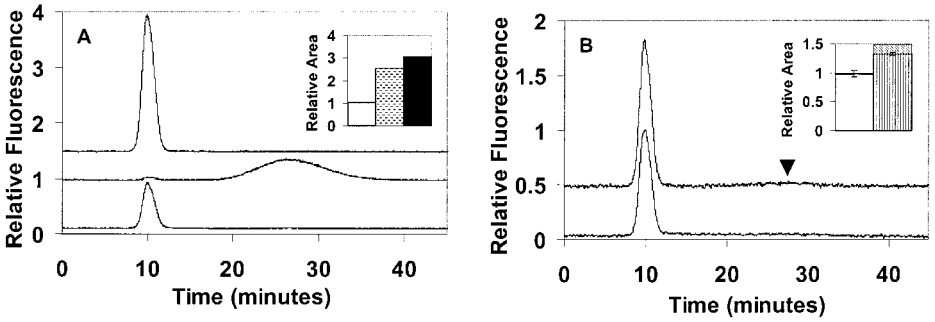

FIGURE 4: Analysis of the egg PG vesicle population before and after permeabilization with protofibrils shows that significant lysis has not occurred. Vesicles (100 nm) were incubated with sample as in Figure 3 for 30 min and then immediately injected onto a gel filtration column. In (A) and (B) the bottom chromatogram represents intact Fura-2-containing vesicles after incubation with buffer alone, while the upper trace in (A) represents the same vesicles after complete permeabilization with 31 nM ionomycin. The middle trace in (A) results from complete lysis of the vesicles with Triton X-100 (0.5%, with sonication for 1 min). The upper trace in (B) results from treatment of Fura-2-containing PG vesicles with 4 μM protofibrillar α-synuclein (see Figure 3, panel A). The heights of the bars in the insets of (A) and (B) represent the relative areas of peaks: white, buffer; dashed, Triton X-100; black, ionomycin; hatched, protofibril. In (A), both treatments allowed recovery of close to the expected theoretical maximum fluorescence (3-fold enhancement), whether it be in the intact vesicle fraction (upper trace) or in the free calcium-complexed Fura-2 (middle trace). The white and hatched bars in (B) represent the average of six and three measurements of blank and protofibril incubations, respectively (the error bars are ±1 standard deviation in size). The hatched bar in (B) represents the fluorescence of two peaks: the void volume peak, representing intact vesicles, with vertical stripes and the free calcium−Fura-2 peak (see arrowhead) with diagonal stripes.

bound protofibril retains its β-sheet-rich structure (Figure 1). Binding of α-synuclein to brain-derived vesicles is highly selective for the protofibrillar form (Lee et al., unpublished results). Finally, the two species affect membrane integrity differently; protofibrillar α-synuclein causes significant permeabilization, while an equal amount of monomeric α-synuclein has no effect. Protofibrillar α-synuclein, but not the monomer, affects the integrity of mica-adsorbed membranes.

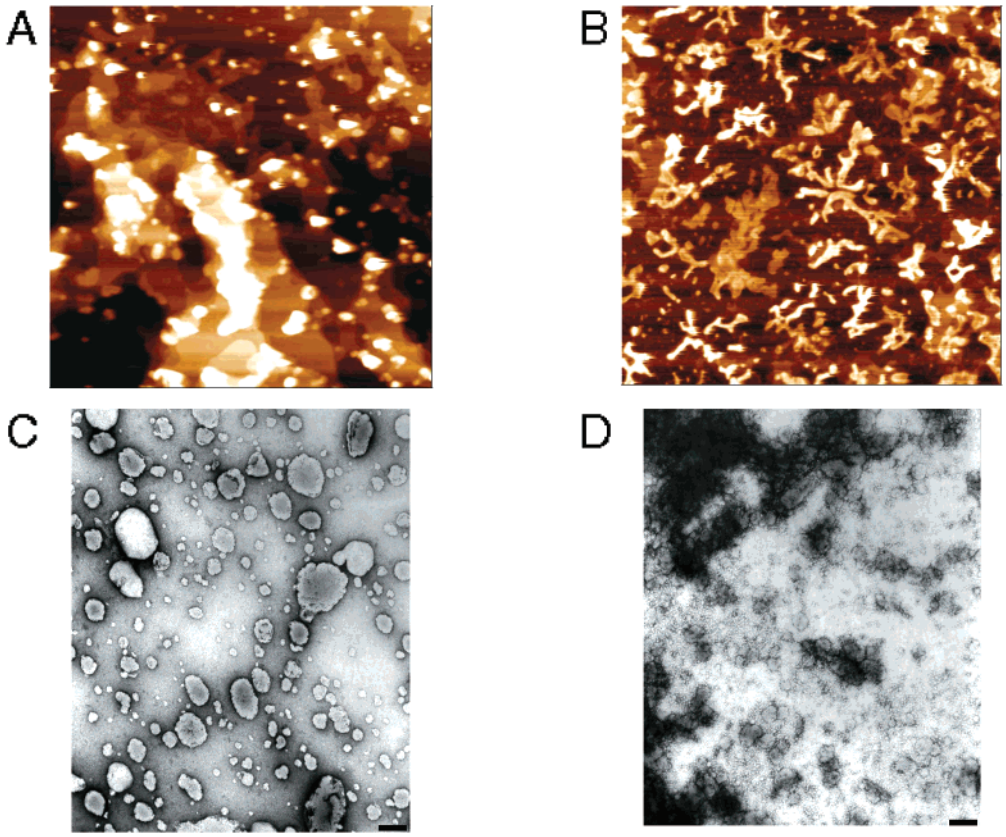

FIGURE 5: AFM and EM images show membrane perturbation by protofibrillar α-synuclein. Mica-adsorbed egg PG vesicles (5 μm^2 images) were incubated with 100 μM α-synuclein before (A) or after (B) incubation for 9 days at 37 °C, conditions known to produce protofibrils. In the presence of monomer (or buffer), large layered structures deposited on the mica surface together with what appears to be lipid vesicles of varied sizes were unperturbed (A). (B) shows a representative field after treatment of adsorbed vesicles with preincubated α-synuclein. (C) and (D) are EM images of egg PG vesicles incubated with buffer or protofibrillar α-synuclein (17 μM), respectively. The black bar in each image represents a length of 200 nm.

Thus vesicle permeabilization fits the primary criterion that a reasonable toxic mechanism must be specifically associated with the protofibrillar form. In addition, the disease-linked mutations have been demonstrated to promote formation of protofibrillar populations (*14*), so mutations could increase the "dose" of the toxic species. In addition, the mutations could promote formation of an *active* protofibril subfraction, the nature of which has not been determined.

Protofibril-induced membrane permeabilization may occur by one of two mechanisms that are utilized by evolved pore-forming protein toxins. First, the antibacterial peptides magainin and cecropin cause transient "pore" formation by localized membrane destruction and micellization, followed by rapid reestablishment of the bilayer (*27*). Second, α-hemolysin (*32*), latrotoxin (*33*), and aerolysin (*34*) all form well-ordered, oligomeric membrane-spanning pores characterized by β-sheet structure. It is important to emphasize that these two classes of membrane-permeabilizing toxins have been optimized for selective cytotoxicity. In contrast, formation of the toxic form of α-synuclein is likely to have been selected *against* by evolution and is merely a consequence of the fact that protofibrils are intermediates in the pathway to stable, albeit potentially biologically inert, amyloid fibrils (*35*, *36*).

Inappropriate membrane permeabilization by protofibrillar α-synuclein could cause the degeneration and death of neurons in several ways (Figure 6) that are consistent with the rate (*37*) and cell-type selectivity (certain membrane compositions may be more susceptible; PG was chosen as a model system but is unlikely to be a major component of the actual target membrane) of PD cell death (*38*). Permeabilization could cause (among other possibilities) (i) unregulated calcium flux into the cytosol (*39*), (ii) depolarization of the mitochondrial membrane (*40*), or (iii) leakage of dopamine into the cytoplasm (note that dopamine is smaller than Fura-2) (Figure 6). Elevation of cytoplasmic dopamine leads to cell death (*41*).

Membrane permeabilization by protofibrillar intermediates could explain the toxicity of other amyloid proteins. This toxicity similarly may not derive from their fibrillar forms, as originally proposed (*42*, *43*), but rather from nonfibrillar oligomeric species whose formation is *linked* to fibrillization (*44*, *45*). Pore-like activity of Aβ (*46*) has been described, and a link between Aβ oligomerization and fluidization/disruption of membranes has been reported (*47*). A similar link was reported for IAPP (*48*). In addition, the formation of an IAPP calcium "channel" (*49*) has been suggested to be oligomerization-dependent.

The model presented in Figure 6 can be tested by perturbing the proposed pathogenic process in vivo (*18*) using sequence changes and drug-like molecules. For example, molecules (or mutations) that prevent the protofibril-to-fibril transition in vitro should, according to the model presented here, accelerate disease progression (but *inhibit* Lewy body formation) in the *Drosophila* model (*8*). Conversely, molecules or mutations that inhibit the monomer-to-protofibril

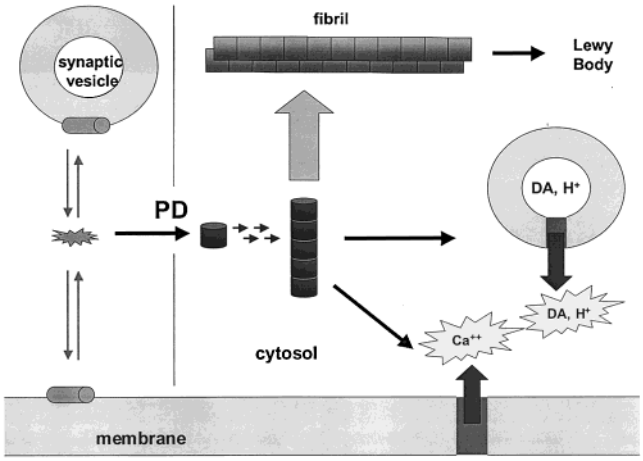

FIGURE 6: The link between α-synuclein fibrillization and PD neurotoxicity may involve inappropriate membrane permeabilization by a protofibrillar species. In the normal cytosol natively unfolded α-synuclein interacts with membranes, including synaptic vesicles, via a helical structure. However, if the critical concentration of α-synuclein is exceeded or if a mutation lowers the critical concentration, ordered β-sheet oligomerization can occur (via the PD pathway), proceeding downhill in an energetic sense to the amyloid fibril (not to scale). Early in this process, protofibrils (cylinders) are transiently populated. As reported here, protofibrils may permeabilize cellular membranes, with deleterious consequences to the neuron. Because the rates of the monomer-to-protofibril (toxin-producing) and the protofibril-to-fibril (toxin-consuming) transitions could be independently influenced by many factors, there may not be a quantitative correlation between cell death and fibrillar LBs.

transition should inhibit disease progression (*and* Lewy body formation). Compounds that inhibit the conversion of monomer to protofibril could be novel therapeutics against Parkinson's disease.

ACKNOWLEDGMENT

We thank John Collier, Mel Feany, Ken Kosik, and Michael Schlossmacher for insightful comments and Harold Scheraga for generously providing us with the Kratos fluorescence detector.

REFERENCES

1. Maroteaux, L., Campanelli, J. T., and Scheller, R. H. (1988) *J. Neurosci. 8*, 2804−2815.
2. Polymeropoulos, M. H., Lavedan, C., Leroy, E., Ide, S. E., Dehejia, A., Dutra, A., Pike, B., Root, H., Rubenstein, J., Boyer, R., Stenroos, E. S., Chandrasekharappa, S., Athanassiadou, A., Papapetropoulos, T., Johnson, W. G., Lazzarini, A. M., Duvoisin, R. C., Di Iorio, G., Golbe, L. I., and Nussbaum, R. L. (1997) *Science 276*, 2045−2047.
3. Kruger, R., Kuhn, W., Muller, T., Woitalla, D., Graeber, M., Kosel, S., Przuntek, H., Epplen, J. T., Schols, L., and Riess, O. (1998) *Nat. Genet. 18*, 106−108.
4. Papadimitriou, A., Veletza, V., Hadjigeorgiou, G. M., Patrikiou, A., Hirano, M., and Anastasopoulos, I. (1999) *Neurology 52*, 651−654.
5. Spillantini, M. G., Schmidt, M. L., Lee, V. M., Trojanowski, J. Q., Jakes, R., and Goedert, M. (1997) *Nature 388*, 839−840.
6. Spillantini, M. G., Crowther, R. A., Jakes, R., Hasegawa, M., and Goedert, M. (1998) *Proc. Natl. Acad. Sci. U.S.A. 95*, 6469−6473.
7. Baba, M., Nakajo, S., Tu, P. H., Tomita, T., Nakaya, K., Lee, V. M.-Y., Trojanowski, J. Q., and Iwatsubo, T. (1998) *Am. J. Pathol. 152*, 879−884.
8. Feany, M. B., and Bender, W. W. (2000) *Nature 404*, 394−398.
9. Masliah, E., Rockenstein, E., Veinbergs, I., Mallory, M., Hashimoto, M., Takeda, A., Sagara, Y., Sisk, A., and Mucke, L. (2000) *Science 287*, 1265−1269.
10. Abeliovich, A., Schmitz, Y., Farinas, I., Choi-Lundberg, D., Ho, W. H., Castillo, P. E., Shinsky, N., Verdugo, J. M., Armanini, M., Ryan, A., Hynes, M., Phillips, H., Sulzer, D., and Rosenthal, A. (2000) *Neuron 25*, 239−252.
11. Dawson, V. L. (2000) *Science 288*, 631−632.
12. Conway, K. A., Harper, J. D., and Lansbury, P. T., Jr. (2000) *Biochemistry 39*, 2552−2563.
13. Conway, K. A., Harper, J. D., and Lansbury, P. T., Jr. (1998) *Nat. Med. 4*, 1318−1320.
14. Conway, K. A., Lee, S. J., Rochet, J. C., Ding, T. T., Williamson, R. E., and Lansbury, P. T., Jr. (2000) *Proc. Natl. Acad. Sci. U.S.A. 97*, 571−576.
15. Narhi, L., Wood, S. J., Steavenson, S., Jiang, Y., Wu, G. M., Anafi, D., Kaufman, S. A., Martin, F., Sitney, K., Denis, P., Louis, J. C., Wypych, J., Biere, A. L., and Citron, M. (1999) *J. Biol. Chem. 274*, 9843−9846.
16. Giasson, B. I., Uryu, K., Trojanowski, J. Q., and Lee, V. M. Y. (1999) *J. Biol. Chem. 274*, 7619−7622.
17. Wood, S. J., Wypych, J., Steavenson, S., Louis, J. C., Citron, M., and Biere, A. L. (1999) *J. Biol. Chem. 274*, 19509−19512.
18. Goldberg, M. S., and Lansbury, P. T., Jr. (2000) *Nat. Cell Biol. 2*, E115−E119.
19. Olson, F., Hunt, C. A., Szoka, F. C., Vail, W. J., and Papahadjopoulos, D. (1979) *Biochim. Biophys. Acta 557*, 9−23.
20. Brown, D. A., and Rose, J. K. (1992) *Cell 68*, 533−544.
21. Lee, S. J., Liyanage, U., Bickel, P. E., Xia, W., Lansbury, P. T., Jr., and Kosik, K. S. (1998) *Nat. Med. 4*, 730−734.
22. Cooper, M. A., Hansson, A., Lofas, S., and Williams, D. H. (2000) *Anal. Biochem. 277*, 196−205.
23. Blau, L., and Weissmann, G. (1988) *Biochemistry 27*, 5661−5666.
24. Weinreb, P. H., Zhen, W., Poon, A. W., Conway, K. A., and Lansbury, P. T., Jr. (1996) *Biochemistry 35*, 13709−13715.
25. Rochet, J. C., Conway, K. A., and Lansbury, P. T., Jr. (2000) *Biochemistry 39*, 10619−10626.
26. Davidson, W. S., Jonas, A., Clayton, D. F., and George, J. M. (1998) *J. Biol. Chem. 273*, 9443−9449.
27. Oren, Z., and Shai, Y. (1998) *Biopolymers 47*, 451−463.
28. Jo, E., McLaurin, J., Yip, C. M., St. George-Hyslop, P., and Fraser, P. E. (2000) *J. Biol. Chem. 275*, 34328−34334.
29. Forloni, G., Bertani, I., Calella, A. M., Thaler, F., and Invernizzi, R. (2000) *Ann. Neurol. 47*, 632−640.
30. Tompkins, M. M., and Hill, W. D. (1997) *Brain Res. 775*, 24−29.
31. Jensen, P. H., Nielsen, M. S., Jakes, R., Dotti, C. G., and Goedert, M. (1998) *J. Biol. Chem. 273*, 26292−26294.
32. Song, L., Hobaugh, M. R., Shustak, C., Cheley, S., Bayley, H., and Gouaux, J. E. (1996) *Science 274*, 1859−1866.
33. Orlova, E. V., Rahman, M. A., Gowen, B., Volynski, K. E., Ashton, A. C., Manser, C., van Heel, M., and Ushkaryov, Y. A. (2000) *Nat. Struct. Biol. 7*, 48−53.
34. Gouaux, E. (1997) *Curr. Opin. Struct. Biol. 7*, 566−573.
35. Chiti, F., Webster, P., Taddei, N., Clark, A., Stefani, M., Ramponi, G., and Dobson, C. M. (1999) *Proc. Natl. Acad. Sci. U.S.A. 96*, 3590−3594.
36. Lansbury, P. T., Jr. (1999) *Proc. Natl. Acad. Sci. U.S.A. 96*, 3342−3344.
37. Clarke, G., Collins, R. A., Leavitt, B. R., Andrews, D. F., Hayden, M. R., Lumsden, C. J., and McInnes, R. R. (2000) *Nature 406*, 195−199.
38. Olanow, C. W., and Tatton, W. G. (1999) *Annu. Rev. Neurosci. 22*, 123−144.
39. Nicotera, P., and Orrenius, S. (1998) *Cell Calcium 23*, 173−180.
40. Budihardjo, I., Oliver, H., Lutter, M., Luo, X., and Wang, X. (1999) *Annu. Rev. Cell Dev. Biol. 15*, 269−290.

41. Ziv, I., Offen, D., Barzilai, A., Haviv, R., Stein, R., Zilkha-Falb, R., Shirvan, A., and Melamed, E. (1997) *J. Neural. Transm., Suppl. 49*, 195−202.
42. Lorenzo, A., and Yankner, B. A. (1994) *Proc. Natl. Acad. Sci. U.S.A. 91*, 12243−12247.
43. Lorenzo, A., Razzaboni, B., Weir, G. C., and Yankner, B. A. (1994) *Nature 368*, 756−760.
44. Hartley, D. M., Walsh, D. M., Ye, C. P., Diehl, T., Vasquez, S., Vassilev, P. M., Teplow, D. B., and Selkoe, D. J. (1999) *J. Neurosci. 19*, 8876−8884.
45. Lambert, M. P., Barlow, A. K., Chromy, B. A., Edwards, C., Freed, R., Liosatos, M., Morgan, T. E., Rozovsky, I., Trommer, B., Viola, K. L., Wals, P., Zhang, C., Finch, C. E., Krafft, G. A., and Klein, W. L. (1998) *Proc. Natl. Acad. Sci. U.S.A. 95*, 6448−6453.
46. Kawahara, M., Kuroda, Y., Arispe, N., and Rojas, E. (2000) *J. Biol. Chem. 275*, 14077−14083.
47. Kremer, J. J., Pallitto, M. M., Sklansky, D. J., and Murphy, R. M. (2000) *Biochemistry 39*, 10309−10318.
48. Janson, J., Ashley, R. H., Harrison, D., McIntyre, S., and Butler, P. C. (1999) *Diabetes 48*, 491−498.
49. Hirakura, Y., Yiu, W. W., Yamamoto, A., and Kagan, B. L. (2000) *Amyloid 7*, 194−199.

BI0102398